International Journal of Automation and Control

ISSN online: 1740-7524 - ISSN print: 1740-7516
https://www.inderscience.com/ijaac

Machine learning-based fault estimation of nonlinear descriptor systems

Tigmanshu Patel, M.S. Rao, Dhrumil Gandhi, Jalesh L. Purohit, V.A. Shah

DOI: 10.1504/IJAAC.2024.10055128

Article History:

Received:	06 August 2022
Last revised:	17 December 2022
Accepted:	10 February 2023
Published online:	30 November 2023

Machine learning-based fault estimation of nonlinear descriptor systems

Tigmanshu Patel

Department of Instrumentation and Control Engineering,
Faculty of Technology,
Dharmsinh Desai University,
Nadiad 387001, Gujarat, India
Email: tigmanshupatel@gmail.com

M.S. Rao*, Dhrumil Gandhi and
Jalesh L. Purohit

Department of Chemical Engineering,
Faculty of Technology,
Dharmsinh Desai University,
Nadiad 387001, Gujarat, India
Email: msrao@ddu.ac.in
Email: dhrumilgandhi.ch@ddu.ac.in
Email: jalesh.purohit@gmail.com
*Corresponding author

V.A. Shah

Department of Instrumentation and Control Engineering,
Faculty of Technology,
Dharmsinh Desai University,
Nadiad 387001, Gujarat, India
Email: vashahin2010@gmail.com

Abstract: This article focuses on the problem of fault estimation of nonlinear descriptor systems (NLDS) using intelligent approaches. Firstly, an extended Kalman filter for descriptor systems is employed for state estimation. Then, the residuals are generated and mapped to detect and confirm the fault. Finally, machine learning approach and neural network models are used to estimate faults. For machine learning approach, Gaussian process regression is employed to estimate fault magnitude. Additionally, a back propagation neural network is also applied for fault estimation. The efficacy of the proposed methods are demonstrated with the help of benchmark chemical mixing tank descriptor system (Yeu et al., 2008) and two-phase reactor and condenser with recycle (Kumar and Daoutidis, 1996). It is observed that the Gaussian process approach outperforms neural network-based approach for fault estimation.

Keywords: descriptor systems; differential algebraic equations; DAEs; fault detection; fault diagnosis; fault estimation.

Reference to this paper should be made as follows: Patel, T., Rao, M.S., Gandhi, D., Purohit, J.L. and Shah, V.A. (2024) 'Machine learning-based fault estimation of nonlinear descriptor systems', *Int. J. Automation and Control*, Vol. 18, No. 1, pp.1–29.

Biographical notes: Tigmanshu Patel is an Instrumentation and Control Engineer who holds a Bachelor's degree with a Gold Medal in Instrumentation and Control Engineering from the Dharmsinh Desai University, and a Master's in Instrumentation and Control Engineering with a specialisation in Control and Automation from the Nirma University. He has conducted research on state estimation and fault diagnosis, with additional research interests in system modelling, process control, and machine learning applications to systems and control. He has presented conference papers, published journal articles and has received awards/scholarships, including EUCA Travel Grant, QUTPRA Scholarship, Top 100 Meritorious Students Across India, etc. He currently serves as an Assistant Professor at Dharmsinh Desai University.

M.S. Rao obtained his BTech from the JNTU College engineering Anantapur, MTech from the M.S. University of Baroda and PhD from the IIT Bombay. He received his 'Excellence in Research' Award for his PhD thesis at the IIT Bombay. He has supervised six PhD projects and guided more than 50 MTech projects. He has published/presented more than 100 research papers. He has successfully completed more than 200 industrial consultancy/research/audit projects. He was elected twice and also served as treasurer of IIChE national executive counsel. He has more than 25 years of teaching/industrial experience. At present eight students are pursuing their PhD under his guidance. Presently, he is working as the Head of Chemical Engineering Department at the Dharmsinh Desai University Nadiad.

Dhrumil Gandhi is a Chemical Engineer with over five years of academic experience. He obtained his Bachelor's degree in Chemical Engineering from the Dharmsinh Desai University in 2014 and went on to pursue his Master's in Chemical Engineering from the BITS-Pilani. His research has centered on the state estimation and fault diagnosis of multi-rate systems, an important part of the fault-tolerant control framework. He is interested in state estimation, system modeling, process control, and fault detection and diagnosis. Currently, he is an Assistant Professor at the Dharmsinh Desai University, where he continues to engage in research and teaching in the domain of chemical engineering.

Jalesh L. Purohit is currently working as a Professor in the Chemical Engineering Department, Dharmsinh Desai University, Nadiad located in a State of Gujarat, India. He received his Bachelor of Engineering in Chemical Engineering from the Gujarat University in 1995, Master of Engineering degree in Chemical Engineering from DDIT (Deemed to be University) in 2003 and PhD from the IIT (Bombay) in 2014. He is having more than 20 years of teaching experience. His research interests are nonlinear dynamics and multiplicity analysis, observer-based estimation and optimal control (MPC/NMPC) of systems described by differential – algebraic equations.

V.A. Shah has received his BE in Instrumentation and Control Engineering from the Gujarat University, Ahmedabad, India, in 1991 and ME in Electrical Engineering (Microprocessor Systems and Applications) from the Maharaja Sayajirao University, Vadodara, India in 1995 and PhD in Instrumentation and Control Engineering from the Dharmsinh Desai University, Nadiad, India, in 2006. He is a currently working as the Dean at the Faculty of Technology, a Professor and the Head at the Department of Instrumentation and Control Engineering, Dharmsinh Desai University, Nadiad, India. He has presented more than 100 national and international conference papers as well as published many journal research papers. He has guided more than 45 MTech. dissertations and guided 12 PhD students. He has reviewed more than 250 national and international conference and journal research papers. His research interests include robotics, embedded systems, advanced process control, fault-tolerant control, designing artificial intelligence-based system and its applications.

1 Introduction

In today's world, a multitude of technologically complex systems are sporadically subject to faults which might result into catastrophic consequences (Li, 2016) for personnel, system and environment. A fault may occur in a system due to improper operation, usage, mounting, non-adherence to limits, ageing and unsuitable operating environment of system component/s or its subsystems. A closed-loop control action may also hide a fault from being observed (Blanke et al., 2001). On account of this, the stability and performance of the closed loop system may degrade or may even result in unforeseen consequences; causing economical loss or industrial accidents where damage, injury or loss of life may occur as evident from historical incidents like Chernobyl plant accident, Bhopal gas tragedy, etc. (Li, 2016). In order to prevent such industrial accidents, reliable control systems can be attained by appropriate fault diagnosis and control either by analytical redundancy or redundant hardware which enables a system to take necessary actions in presence of fault/s. The control action applied in such situations can diminish the risk as well as ensure nominal operation of the process/system until next shutdown. This control effort largely depends upon the type and magnitude of the fault. Thus, fault diagnosis play a critical role in the fault tolerant control framework which can prevent life-hazards or industrial accidents by acting in a timely manner.

The fault diagnosis methods are generally classified as system model-based, signal-based or knowledge-based methods. A variety of systems can be conveniently modelled in descriptor/differential algebraic equation (DAE) form. Such systems include chemical processes, power systems, electrical circuits, mechanical systems, thermodynamic processes, water distribution networks, vehicle dynamics, etc. These systems require deliberate approaches to address peculiar issues such as requirement of some variables to be differentiable, consistent initialisation, etc. unlike conventional ordinary differential equation (ODE) systems. Descriptor systems tend to show impulsive behaviour for arbitrary initial conditions while numerical methods can fail if certain variables are not differentiable. On the other hand, such systems can be converted to ODEs but they eventually result into numerical errors (Mandela et al.,

2010). Additionally, the resultant system will possess canonical variables that might not have any physical significance. Hence, these systems are considerably different than conventional state space systems and need to be dealt with explicitly.

The fault diagnosis as well as fault tolerant control methods (Zhang and Jiang, 2003; Zhang et al., 2002, 2008; Das et al., 2014; Iqbal et al., 2019; Wu et al., 2011; Isermann, 2005) have been well developed for conventional system representations. While majority of works (Zhang et al., 2002, 2008; Das et al., 2014; Iqbal et al., 2019) have focused on conventional state space systems, the problem of fault diagnosis for descriptor systems is not investigated thoroughly. Additionally, such studies tend to focus on issues of fault detection and isolation and sometimes seem to discount the importance of fault estimation. On the other hand, majority of works (Qiao et al., 2017; Sjöberg, 2006; Rao et al., 2003; Masubuchi et al., 1997) exhibit considerable interest in research on identification and control of descriptor systems. However, many areas pertaining to fault diagnosis of descriptor systems have received minimal attention. It is observed that the problem of fault detection and isolation (Patel et al., 2019; Taqvi et al., 2018; Hamdi et al., 2012; Alkov and Weidemann, 2013; Huang et al., 2003; Patel et al., 2020b) of descriptor systems has been addressed frequently and well studied. On the other hand the fault estimation of NLDS has been analysed by various approaches based on observers in frequency domain (Chan et al., 2019a), sliding mode observers (Chan et al., 2019b, 2019c) recently to other approaches that rely on simultaneous state and fault estimation (Witczak et al., 2016; Shi and Patton, 2014) or dedicated observers that utilise a multi-model approach (Jia et al., 2015; Wang et al., 2013). Of these, some works (Chan et al., 2019a; Witczak et al., 2016; Shi and Patton, 2014; Jia et al., 2015) for descriptor systems which focus on fault estimation by dedicated observer or augmented observer design require linear matrix inequality (LMI)-based approaches to determine observer gains for fault estimation. In this design methodology, the problem needs to be cast or recast as semi-definite programming (SDP) problems which at times can be an inconvenient process. Moreover, the problem of fault estimation for descriptor systems which draws upon powerful and modern methods based on artificial intelligence (AI) has rarely been addressed except for few investigations (Wang et al., 2014; Vemuri et al., 2001) and hence requires critical attention. Recently, the status of machine learning algorithms for processing large amounts of data, application issues and challenges are discussed (Wang et al., 2022). The fault estimation which is an integral component of fault diagnosis is a challenging issue that has been addressed by some researchers (Sun et al., 2021; Qi et al., 2018). The use of deep learning techniques, including artificial neural networks, recurrent neural networks, and other machine learning models to directly model the relationship between the input and output is discussed. In Sun et al. (2021), the performance of soft computing-based approaches for fault diagnosis is evaluated and analysed comparatively. These techniques have the advantage of handling complex nonlinear relationships, and they have demonstrated superiority over traditional methods in various applications.

The investigation carried out in this paper derives its motivation from various works (Vemuri et al., 2001; Wang et al., 2014) which are applied for fault diagnosis as well as other most recent works (Lee et al., 2018; Myren and Lawrence, 2021; Fugh et al., 2022) that dissect the topic of Gaussian processes, however, limited to the domain of machine learning. In this study, we hereby evaluate two different approaches for fault estimation of nonlinear descriptor system (NLDS). These approaches are based on back propagation neural networks and Gaussian processes that rely on a common

dataset for modelling/training respectively. It is worthy to mention that the machine learning-based approach for fault estimation shown in this work is rarely assessed in any study. The approaches employed in this study differ from the methods applied in various investigations. In Vemuri et al. (2001), an online approximator in the form of sigmoidal neural networks is employed for fault diagnosis of linear descriptor systems. It assumes that the state variables are readily available. Additionally, in contrast to Vemuri et al. (2001), the approaches for fault estimation in this study is only dependent on residual information. In Wang et al. (2014), a radial basis function (RBF) neural network is implemented to model actuator faults for a class of NLDSs which is further estimated by an adaptive observer. In that, the neural network is not directly involved in the process of fault estimation itself but it is utilised to represent the fault. For the approach considered in this work, the neural network explicitly performs the function of fault estimation. It should be noted that fault estimation is a non-trivial problem since the output is fault magnitude unlike fault detection and isolation which provides information only in qualitative terms. Further, the technique of fault estimation proposed on Bayesian approach of machine learning has rarely been employed for fault estimation of NLDSs. Thus, the proposed approaches are in stark contrast with earlier works.

The rest of the article is organised as follows. In the next section, we first describe the approach of fault detection based on residual generation and evaluation. In the subsequent sections, we describe the methods of fault estimation. Lastly, these approaches are implemented on a chemical mixing tank NLDS (Yeu et al., 2008) and two phase reactor and condenser with recycle (Kumar and Daoutidis, 1996) for which the results of fault estimation are put forth.

2 Fault detection

In order to detect the occurrence of fault, the residual signal is required (Mohanty et al., 2012; Singhal et al., 2022; Kantharia et al., 2014; Kamdar et al., 2015; Patel et al., 2019, 2020a, 2020b, 2013). Since the residual signal can be generated from the knowledge of state estimates, the state estimation approach avails the use of an extended Kalman filter (Mandela et al., 2010) for NLDSs. Several modifications of the same are further studied (Patel et al., 2020a; Purohit and Patwardhan, 2018). The EKF filter for descriptor systems (Mandela et al., 2010) is featured briefly by block diagram presented in Figure 1 and the necessary details of the same are put forth.

Consider a NLDS with sampling time Δt expressed as

$$\begin{aligned} \hat{x}_{k+1} &= \hat{x}_k + \int_{k\Delta T}^{(k+1)\Delta t} f(x(t), z(t))dt + w_{k+1} \\ g(x(t), z(t)) &= 0, \ k\Delta T \leq t \leq (k+1)\Delta t \end{aligned} \tag{1}$$

where $x \in R^{n-r}$ is differential state, $\hat{x}$ is estimated differential state, $z \in R^r$ is algebraic state and the function $g(x(t), z(t))$ defines algebraic constraints. As shown in Figure 1, the algebraic constraints are employed by constraint solver block in the process of algebraic state estimation. It can be easily perceived that $\begin{bmatrix} x \\ z \end{bmatrix}$ is descriptor state vector.

Additionally, w_{k+1} is process noise with zero mean and known covariance given by matrix Q. The system output as a function of descriptor state vector can be given as

$$y_{k+1} = h(x_{k+1}, z_{k+1}) + v_{k+1} \tag{2}$$

where v_{k+1} is measurement noise with zero mean and known covariance matrix R, h is the measurement model and y is system output/s. For the given system expressed by equations (1)–(2), the EKF determines the estimate of x_k, i.e., $\hat{x}_k$ and z_k, i.e., $\hat{z}_k$ given the observations y_k along with the knowledge of input and initial states. It should be noted that the system [equations (1)–(2)] eliminates consideration of system input for the sake of simplicity.

Figure 1 Block diagram: EKF for descriptor systems (see online version for colours)

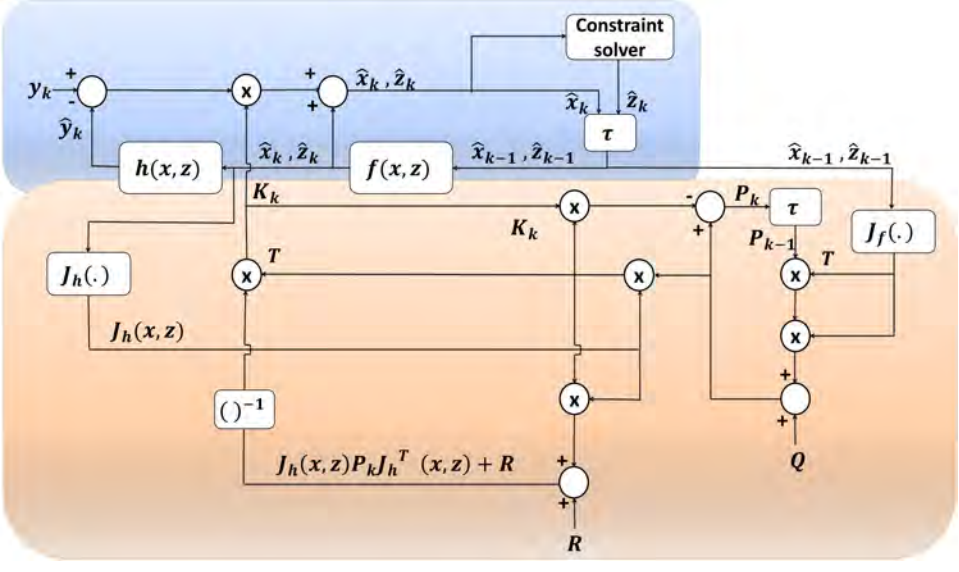

The system expressed above by equation (1) can be linearised as

$$\begin{aligned} \dot{x} &= Ax + Bz \\ 0 &= Cx + Dz \end{aligned} \tag{3}$$

where

$$\begin{bmatrix} A\ B \\ C\ D \end{bmatrix} = \begin{bmatrix} \frac{\partial f}{\partial x} & \frac{\partial f}{\partial z} \\ \frac{\partial g}{\partial x} & \frac{\partial g}{\partial z} \end{bmatrix}$$

From equation (3), the following can be obtained

$$0 = C\dot{x} + D\dot{z} \tag{4}$$

and then rearranged into

$$\dot{z} = -D^{-1}C\dot{x} \tag{5}$$

Since $\dot{x} = Ax + Bz$ the equation (5) yields into

$$\dot{z} = -D^{-1}CAx - D^{-1}CBz \tag{6}$$

which is further used to augment the original system. The augmented system then becomes

$$\begin{bmatrix} \dot{x} \\ \dot{z} \end{bmatrix} = \begin{bmatrix} A & B \\ -D^{-1}CA & -D^{-1}CB \end{bmatrix} \begin{bmatrix} x \\ z \end{bmatrix} \tag{7}$$

for which a brief representation can be

$$\dot{x}^{aug} = A^{aug}x^{aug} \tag{8}$$

where x^{aug} and A^{aug} can be easily inferred from equation (7). The EKF algorithm starts by propagating the descriptor states forward by suitable solver from current time instant to next time instant. The covariance matrix of the augmented states can be given as

$$P_{k+1}^{aug} = \Phi P_k^{aug}\Phi^T + \Gamma Q_{k+1}\Gamma^T \tag{9}$$

where $\Phi = e^{(A^{aug}\Delta t)}$ and $\Gamma = \begin{bmatrix} I \\ -D^{-1}C \end{bmatrix}$.

The Kalman gain is then computed as

$$K_{k+1} = P_{k+1}H_{k+1}^{aug\,T}(H_{k+1}^{aug}P_{k+1}H_{k+1}^{aug\,T} + R)^{-1} \tag{10}$$

Further, the state estimate with the knowledge of Kalman gain and sensor information can be updated as

$$\hat{x}_{k+1} = \hat{x}_{k+1|k} + K_{k+1}(y_{k+1} - h(\hat{x}_{k+1|k}, \hat{z}_{k+1|k})) \tag{11}$$

The correction of state estimates is also displayed in Figure 1 as seen from the top left corner. From the resultant descriptor states, the differential states are retained and utilised to compute the algebraic states by solving the constraint equation as

$$g(\hat{x}_{k+1}, \hat{z}_{k+1}) = 0 \tag{12}$$

which obtains the improved estimate for the algebraic state estimate. The constraint solver shown in Figure 1 represents the same. It also ensures consistent initialisation of solver during next iteration. Finally the covariance matrix P_{k+1}^{aug} is updated as

$$P_{k+1}^{aug} = (I - K_{k+1}^{aug}H_{k+1}^{aug})P_{k+1|k}^{aug} \tag{13}$$

and the EKF filter proceeds to next iteration. Further, the measurement model given by equation (2) is utilised to predict system output from estimated states. Next, the difference between the measured output and estimated output facilitates residual generation. The innovation or residual signal can be expressed as

$$r_i = y_n - \hat{y} \tag{14}$$

where $i \in [1, q]$, $y_n \in R^q$ is measured output/s and $\hat{y} \in R^q$ is predicted output/s. Subsequently, the innovation sequence may then be passed through a filter or mapped using a residual evaluation function. The residual evaluation function employed in this case is a root mean square (RMS) function. The RMS value measures the average energy of the signal over a certain time interval. The RMS value of the signal can be defined as the square root of the mean of the squares of a set of signal magnitude. The RMS value is denoted by $\|.\|_{RMS}$. In case of discrete system for n samples of signal, the RMS value can be given as

$$\|r(k)\|_{RMS} = \sqrt{\frac{1}{n}\left(r_k^2 + r_{k-1}^2 + r_{k-2}^2 \ldots + r_{k-n}^2\right)} \tag{15}$$

which can be briefly represented as

$$\|r(k)\|_{RMS} = \sqrt{\frac{1}{n}\sum_{i=1}^{n} \|r_{k-i}\|^2} \tag{16}$$

Figure 2 Block diagram: fault detection and fault estimation (see online version for colours)

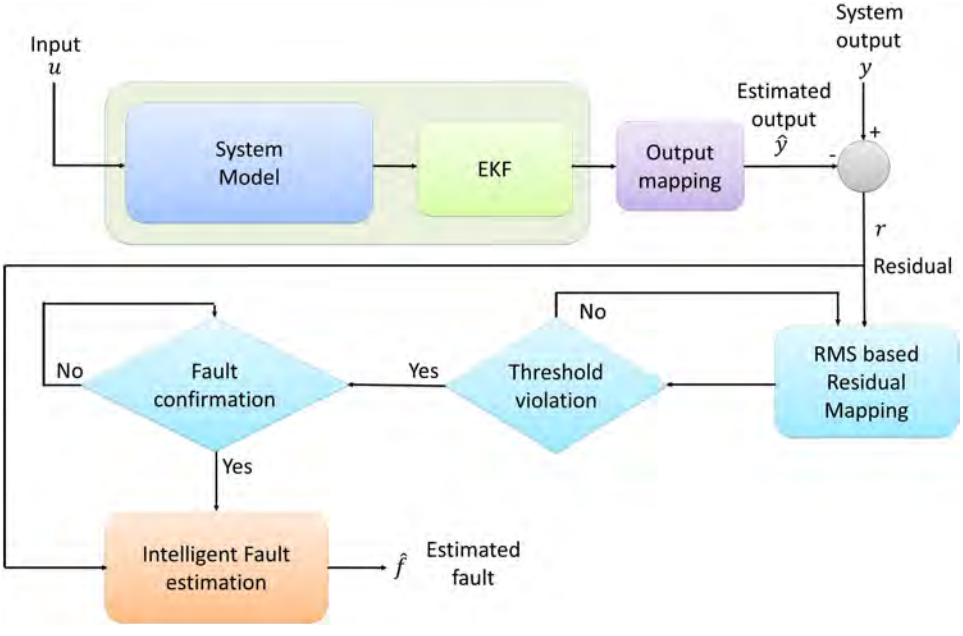

Intuitively, it can be understood as a moving window/buffer that considers sample data points of residual signal from r_k to r_{k-n}; where n is the number of signal samples. The solution to the fault detection problem can be posed as

$$\begin{aligned} &\|r\|_{RMS} < \|r\|_{RMSmin} \text{ or } \|r\|_{RMS} > \|r\|_{RMSmax};\ fault\ detected \\ &\|r\|_{RMSmin} \leq r \leq \|r\|_{RMSmax};\ fault\ free,\ nominal\ operation \end{aligned} \tag{17}$$

such that $\|r\|_{RMSmin}$ and $\|r\|_{RMSmax}$ are minimum and maximum value of $\|r\|_{RMS}$. These minimum and maximum values of residual signal can be determined from nominal system operation. The overall block diagram of the entire process for state estimation, fault detection and fault estimation is presented in Figure 2. In that, the residual is mapped by RMS function and checked whether any thresholds are violated. If any thresholds are exceeded, a window of certain time period is chosen to confirm the fault. During this window, the mapped residual signal should constantly violate respective thresholds in order to confirm the fault. After the existence of fault is confirmed, the fault estimation block is activated to estimate the fault magnitude. As shown in Figure 2, the intelligent fault estimation approach relies only on residual information in order to estimate the fault.

3 Fault estimation

The problem of fault estimation is evaluated thoroughly within this study. In contrast to fault detection, it should be recalled that the problem of fault estimation is complex and critical within framework of fault tolerant control. As shown in Figure 2, upon detection of fault, the fault is confirmed provided that the threshold is continuously violated for certain number of consecutive time instants. Further, the fault estimation module determines the magnitude of the confirmed fault which can be further utilised for control.

The intelligent fault estimation can be realised by a machine learning algorithm that possesses regression capabilities such as linear regression, logistic regression, ridge regression, Lasso regression, Bayesian regression and others. The simplest form of regression is linear regression and can be used to determine the relationship between two variables which is presumably linear. The logistic regression can be opted when the dataset is large such that there is almost equal occurrence of values to predict in target variables. On the other hand, the ridge regression is used when there is a high correlation between the independent variables. In contrast to ridge regression where the regression coefficient value is larger, Lasso regression performs regularisation of regression coefficient along with the advantage of feature selection to build a model. This feature subset prevents over-fitting of the model. Lastly, the Bayesian regression is based on Bayes theorem to determine the value of regression coefficients. In this method of regression, the posterior distribution of the features is determined instead of least-squares approach. Bayesian regression is similar to both linear regression and ridge regression but more stable than the simple linear regression. Thus, Bayesian regression-based approach such as Gaussian process regression (GPR) can be a good choice to establish the relation between residuals and fault magnitude. On the other hand, the neural network-based approach can also be applied to model the relation between different variables. The two approaches considered in this paper, namely, neural network-based approach and GPR-based approach are discussed further.

3.1 Neural network approach

In Vemuri et al. (2001), the neural network-based approach utilises state information along with inputs to estimate the fault. In contrast, the proposed approach relies only on residual information to estimate the fault magnitude. Additionally, Vemuri et al. (2001)

uses a dead zone approach for fault detection which may render itself incapable to detect low magnitude faults. In the proposed approach, the fault isolation scheme activates a pre-trained neural network for fault estimation. A backpropagation neural network (BPNN) alternatively known as multilayer perceptron or Feedforward neural network is employed in this case.

A neural network is made up of simple processing units that can store experiential knowledge and process new information. Consider the neural network of Figure 3. Each neuron within a neural network performs two distinct computations

1 $z = w^T x + b$

2 $a = \sigma(z)$, where w and b are vectors for weights and bias respectively. x is input and $\sigma(z)$ is activation function which is hyperbolic tangent in this case.

Alternatively, a can be expressed as $g(z)$ meaning the same. For a given network of Figure 3, the forward pass can be given as

The forward propagation can be given as

$$\begin{aligned} z^{[1]} &= W^{[1]} x^{(i)} + b^{[1]} \\ a^{[1]} &= g(z^{[1]}) \\ z^{[2]} &= W^{[2]} a^{(1)} + b^{[2]} \\ a^{[2]} &= g(z^{[2]}) \\ z^{[3]} &= W^{[3]} a^{(2)} + b^{[3]} \\ \hat{y}^{(i)} &= a^{[3]} = g(z^{[3]}) \end{aligned} \tag{18}$$

The output $\hat{y}$ from the neural network can be used to determine error with the help of a loss function. The Least squared error is most commonly used loss function and denoted by L. Based on the scalar output from the loss function the following weight update for a certain layer l can be performed

$$W^{[l]} = W^{[l]} - \alpha \frac{\partial L}{\partial W^{[l]}} \tag{19}$$

Similarly,

$$b^{[l]} = b^{[l]} - \alpha \frac{\partial L}{\partial b^{[l]}} \tag{20}$$

where α is the learning rate. In order to perform the above update, the gradients must be found. The backpropagation method can be extended to neural networks of different structures and different sizes. In order to apply this to problem at hand, the residuals and fault magnitude form the dataset. The residuals are the inputs while known fault magnitudes become the targets during the training stage of neural network. After pre-defined number of epochs or no scope of further improvement, the update of the hyper-parameters terminate. The trained model can then be tested with values that were never presented earlier in order to determine the prediction accuracy of the neural network model. If appropriate, the neural network can then be implemented online to determine the fault magnitude for given residuals.

Figure 3 Two layer neural network (see online version for colours)

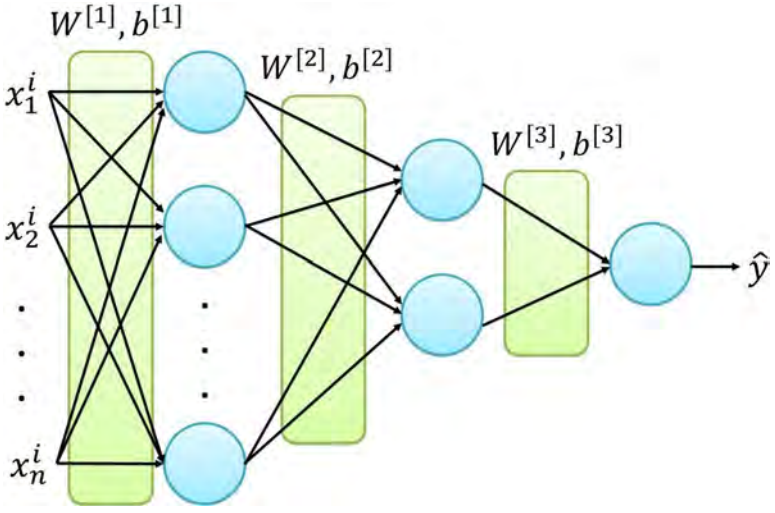

3.2 GPR approach

The machine learning approaches are rarely explored for descriptor systems. In contrast to earlier studies (Iqbal et al., 2019; Kankar et al., 2011), where deep learning (Iqbal et al., 2019) and SVM (Kankar et al., 2011) is employed for fault detection and isolation, the machine learning approach employed in this case relies on Gaussian processes and addresses the issue of fault estimation.

GPR is a powerful, non-parametric Bayesian approach towards regression problems (Schulz et al., 2018). A Gaussian process defines a distribution over functions such that it follows a joint (multivariate) Gaussian distribution. The GPR computes the probability distribution over all admissible functions that fit the given set of data. In GPR, the output y of a function f can be expressed as

$$y = f(x) + \epsilon \tag{21}$$

where x is the input and ϵ is noise such that $\epsilon \sim N(0, \sigma_\epsilon^2)$. Additionaly, the function $f(x)$ is considered to be a random variable which follows a Gaussian process distribution given as

$$f(x) \sim GP(\mu(x), k(x, x')) \tag{22}$$

where x' denotes another data point. The mean function $\mu(x)$ in a way states the expected function value at input x which is the average of all functions evaluated at input x. This can be expressed as

$$\mu(x) = E[f(x)] \tag{23}$$

The prior mean function is mostly set to $\mu(x) = 0$ so as to avoid any expensive posterior computations. Additionally, $k(x, x')$ is covariance function (or kernel function) that captures the dependence between two different input points x and x' given as

$$k(x, x') = E[(f(x) - \mu(x)(f(x') - \mu(x')] \tag{24}$$

There are various options available for the choice of a kernel function such as squared exponential, rational quadratic, exponential kernel, matern 3/2, matern 5/2, etc. One of the most commonly employed kernel is squared exponential which can be expressed as

$$k(x, x') = \sigma_f^2 \exp\left(-\frac{\|x - x'\|^2}{2\lambda^2}\right) \tag{25}$$

In equation (25), the hyper-parameters λ is length scale while σ_f^2 represents signal variance. These hyper-parameters can be varied in order to change the apriori correlation between points.

Now for a given set of data $D = \{X_t, y_t\}$, in order to make predictions for new inputs $\tilde{X}$ by drawing $\tilde{f}$ from the posterior distribution, then the distribution can be given as

$$\begin{bmatrix} y_t \\ \tilde{f} \end{bmatrix} \sim \left(0, \begin{bmatrix} K(X_t, X_t) + \sigma_\epsilon^2 I & K(X_t, \tilde{X}) \\ K(\tilde{X}, X_t) & K(\tilde{X}, \tilde{X}) \end{bmatrix}\right) \tag{26}$$

where K denotes respective covariance matrices between respective points, I is identity matrix.

The conditional distribution $p(\hat{f}|X_t, y_t, \hat{X})$ is then a multivariate normal distribution with mean

$$K(\tilde{X}, X_t)[K(X_t, X_t) + \sigma_\epsilon^2 I]^{-1} y_t \tag{27}$$

and covariance as

$$K(\tilde{X}, \tilde{X}) - K(\tilde{X}, X_t)[K(X_t, X_t) + \sigma_\epsilon^2 I]^{-1} K(X_t, \tilde{X}) \tag{28}$$

It should be noted that the above posterior is also a Gaussian process with mean function

$$\mu_t(x) = K(x, X_t)[K(X_t, X_t) + \sigma_\epsilon^2 I]^{-1} y_t \tag{29}$$

and the kernel is

$$k_t(x, x') = k(x, x') - K(x, X_t)[K(X_t, X_t) + \sigma_\epsilon^2 I]^{-1} K(X_t, x') \tag{30}$$

To predict, the mean of equation (29) or sampled functions from the Gaussian process with this mean function and the kernel expressed by equation (30) can be used. The problem of fault estimation can be viewed as a fault being a function of residuals and modelled to predict the fault magnitude. As discussed, a set of observations can be used to fit a GPR model. This model can then be employed to predict the fault for a given input (residual).

4 Results and discussion

4.1 Case study 1

In order to assess the approaches described earlier, a physical system of chemical mixing tank (Yeu et al., 2008) in descriptor form is considered as depicted by Figure 4. Each mixing tank has standpipe which facilitate for a descriptor system formulation. The system has two inputs (q_1, q_4) which provide inflow of chemical to tank 1 and tank 2 respectively. It has three outputs (q_3, c_5, q_5). On account of standpipes, any excess fluid will overflow and ensures that the heights h_1 and h_2 are constant. Further, the dynamic model of the system can be obtained given as

$$\begin{aligned} V_1\dot{c_3} &= c_1q_1 + c_2q_2 - c_3q_3 \\ V_2\dot{c_5} &= c_3q_3 + c_4q_4 - c_5q_5 \end{aligned} \tag{31}$$

and the equilibrium relations/constraints can be given by

$$\begin{aligned} q_3 &= q_1 + q_2 \\ q_5 &= q_3 + q_4 \end{aligned} \tag{32}$$

Consider the following representation where input, descriptor variables and outputs are denoted by

- Inputs: $u(t) = \begin{bmatrix} u_1\ u_2 \end{bmatrix}^T = \begin{bmatrix} q1\ q4 \end{bmatrix}^T$.
- Descriptor states: $x(t) = \begin{bmatrix} x_1\ x_2\ x_3\ x_4 \end{bmatrix}^T = \begin{bmatrix} c_3\ c_5\ q_3\ q_5 \end{bmatrix}^T$.
- Outputs: $y(t) = \begin{bmatrix} y_1\ y_2\ y_3 \end{bmatrix}^T = \begin{bmatrix} q_3\ c_5\ q_5 \end{bmatrix}^T$.

On utilising the above variable definition in equations (31) and (32), an alternate representation can be obtained as

$$\begin{aligned} V_1\dot{x_1} &= c_1u_1 + c_2q_2 - x_1x_3 \\ V_2\dot{x_2} &= x_1x_3 + c_4u_2 - x_2x_4 \\ u_1 + q_2 - x_3 &= 0 \\ x_3 + u_2 - x_4 &= 0 \end{aligned} \tag{33}$$

Additionally, the system parameters are tabulated in Table 1. Firstly, the results of state estimation for physical system are put forth. The simulation time step is $dt = 1s$ while the system states and estimator states are initialised as $x_0 = x_{0f} = \begin{bmatrix} 0\,0\,0\,0 \end{bmatrix}^T$. The process noise covariance matrix is considered to be $Q = \begin{bmatrix} 0.0025 & 0 \\ 0 & 0.0025 \end{bmatrix}$ while the measurement noise covariance matrix is $R = \begin{bmatrix} 0.01 & 0 & 0 \\ 0 & 0.0025 & 0 \\ 0 & 0 & 0.01 \end{bmatrix}$. Furthermore, the initial error covariance matrix is assumed to be $P_0 = I_{4\times4}$. As evident from the results depicted in Figure 5, the state estimates are in good agreement with the system states. It is also noticeable that the estimated states track the system states even in dynamic conditions.

Figure 4 A chemical mixing tank system

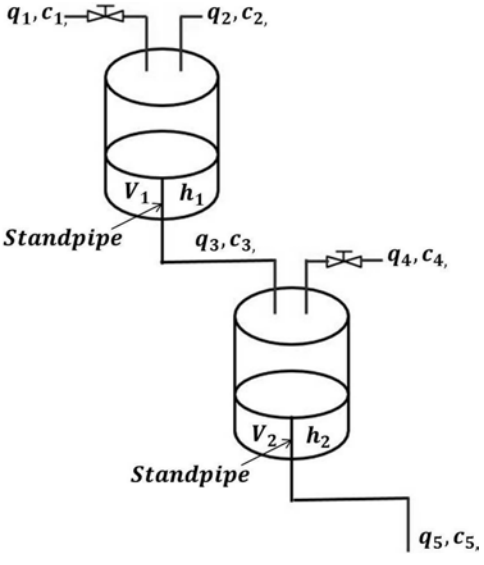

Source: Yeu et al. (2008)

Figure 5 Estimation results for chemical mixing tank NLDS (see online version for colours)

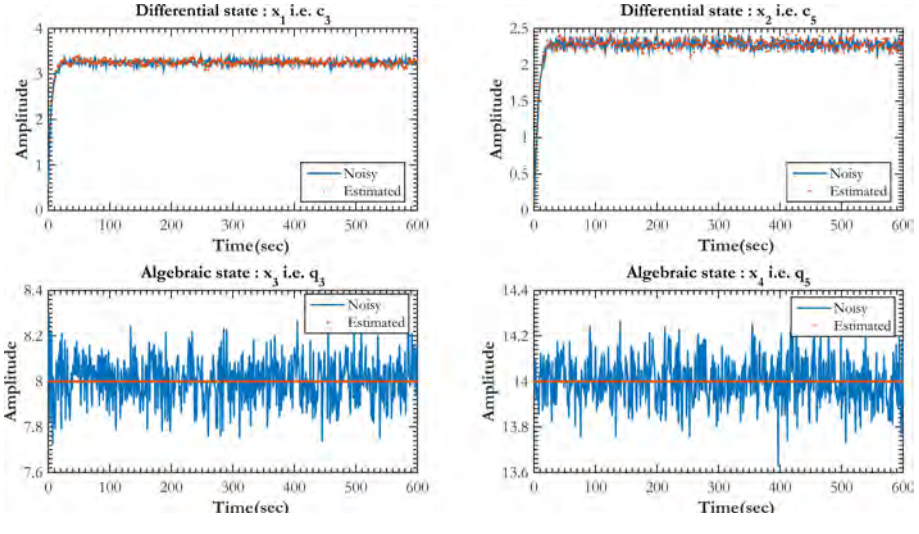

Next, the state estimates are utilised to predict system output that in turn is utilised to generate residuals. The residuals are mapped by a RMS evaluation function. The thresholds are obtained from nominal conditions of system operation. These thresholds are further utilised to assess the problem of fault detection in a brief manner. In this study, a window of $n = 10$ samples was considered for residual evaluation. The thresholds were identified from nominal operating conditions to be $[0.19 \quad 0.06 \quad 0.18]^T$. A fault is detected when any residual evaluation signal violates their respective

threshold. Further, the occurrence of fault is confirmed considering a window of $n = 5$ samples. Now, in order to evaluate fault detection; actuator fault in u_1 is considered. The faults are introduced around time $t = 300$ s for simulation results presented in Figure 6. In Figure 6, the residual evaluation signal is plotted along with respective thresholds for an under-actuation fault in actuator u_1 (of –10%). It should be recalled that $y \in R^3$ and hence $r \in R^3$. All mapped signals continue to remain well within threshold limits before time $t = 300$ s. It should be noticed that the magnitude of the residual evaluation signals are small before $t = 300$ s which implicitly denotes negligible estimation error. As evident in Figure 6, all mapped residual signals suddenly peaks after time $t = 300$ s and violate respective thresholds indicating the occurrence of a fault. The threshold violations stand true consecutively for five time instants which confirm the fault. Thus, the occurrence of fault is detected and confirmed. In order to evaluate the approaches of fault estimation, a dataset is generated which is availed by fault estimation approaches. All of these approaches learn/generate a model from this dataset. The considered approaches are demonstrated on estimation of fault magnitude for a fault that occurs in actuator u_1. In order to do so, the dataset containing residuals and fault magnitude was generated for actuator u_1 wherein discrete fault values with step size of 10 and range of -100% to 100% was considered. Hence, the dataset generation was performed for values as follows: fault in actuator u_1 = [–100% –90% –80% ... 80% 90% 100%]. For each magnitude of fault shown above, a training dataset was generated which consisted of residuals and fault magnitude. The simulation for training dataset generation was carried out for a time horizon of $t = 200$ s where the fault in u_1 was introduced at around $t = 100$ s. The entire training dataset to be presented to respective models was formed by appending all such datasets generated.

Figure 6 Residual evaluation signal vs. threshold: –10% fault in u_1 (see online version for colours)

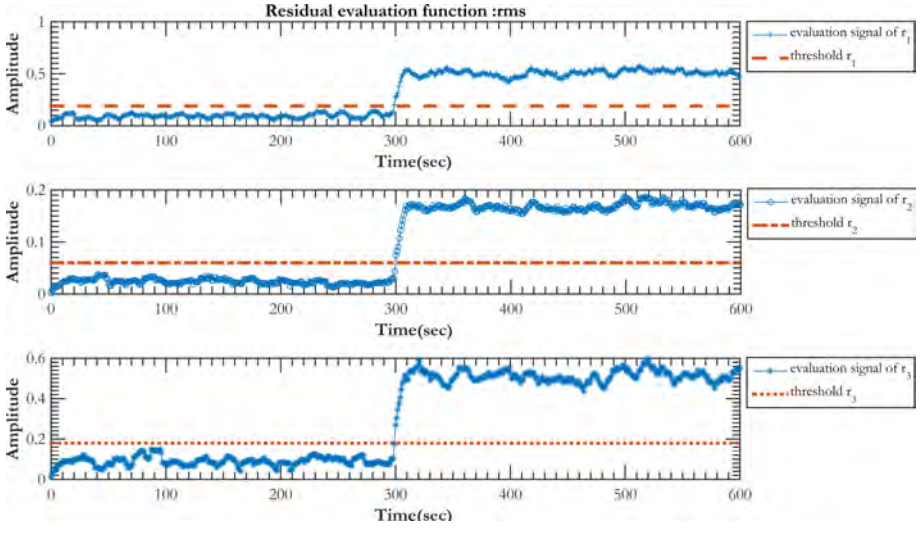

The neural network structure employed for fault estimation is shown in Figure 7 which consists of one input layer, two hidden layers and one output layer wherein the hidden layers consist of five and three neurons respectively. The neural network was trained

with residuals as input and normalised fault magnitudes as outputs. The results of training the neural network depicts R values of 0.9 indicating that the trained model can predict fault magnitudes that are close to actual fault magnitudes.

The trained BPNN is further assessed by applying varying abrupt fault for actuator u_1. A fault of 20% magnitude was introduced in actuator u_1 around time t = 400 s. All fault estimation results presented in this work are continuously averaged over a window of five samples. As evident from Figure 8, the abrupt actuator fault of chemical mixing tank system is tracked by the backpropagation neural network in a satisfactory manner. Additionally, when the fault is constant, the neural network is capable to estimate the fault. In order to assess it further, during another simulation, a fault of –10% magnitude is introduced in u_1 at t = 400 s. The fault estimation results for the same are presented in Figure 9 and found to be satisfactory.

Table 1 System parameters

Concentration of chemical 1 c_1	4 mol/l
Concentration of chemical 2 c_2	2 mol/l
Concentration of chemical 4 c_4	1 mol/l
Volume of liquid in mixing tank 1 V_1	40 l
Volume of liquid in mixing tank 1 V_2	50 l
Input flow rate (steady state) q_1	5 l/s
Input flow rate (steady state) q_4	6 l/s
Flow rate of chemical 2 q_2	3 l/s

Figure 7 Backpropagation neural network structure for fault estimation (for case 1) (see online version for colours)

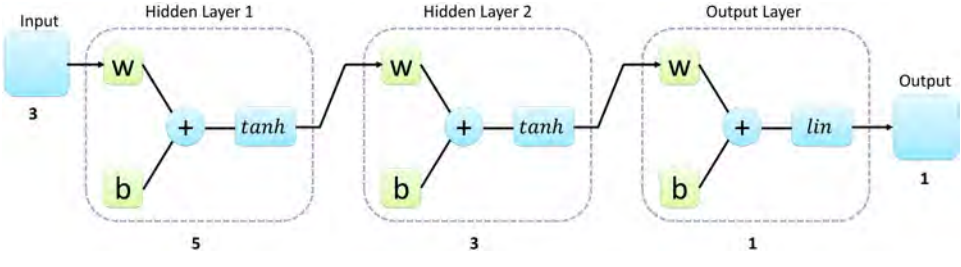

Further, the GPR approach is also analysed for fault estimation. The GPR model is structured to have pure quadratic as basis function while squared exponential as kernel function. As mentioned earlier, the training dataset tends to be the same as utilised earlier in case of backpropagation neural network. For fitting the GPR model, the residuals were provided as inputs and fault magnitudes as expected values. Subsequently, the trained GPR model is then examined for actuator fault estimation of chemical mixing tank system. The results of fault estimation via GPR appraoch is included in Figures 8–9. It can be easily perceived that the fault estimates are in excellent agreement with the actual fault. The GPR-based fault estimation shows superior performance as compared to neural network approach. The backpropagation neural network-based fault estimation approach exhibits some noisy behaviour. In contrast, the fault estimation performance of GPR model is excellent in terms dynamic response as well as fault estimation for constant value of fault.

Figure 8 Actuator (u_1): abrupt fault estimation by NN and GPR approaches (see online version for colours)

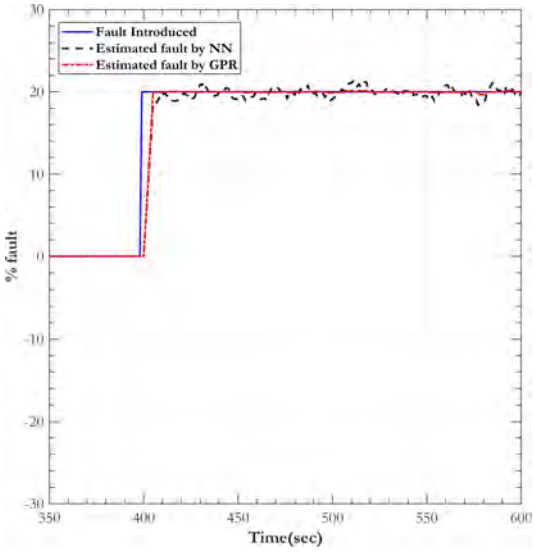

Figure 9 Actuator (u_1): abrupt fault estimation by NN and GPR approaches (see online version for colours)

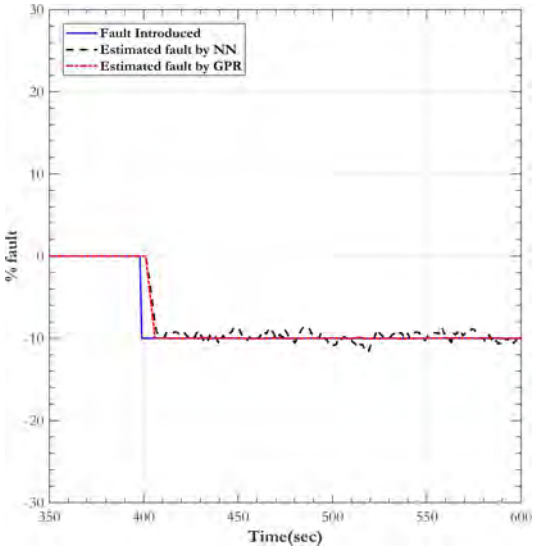

In terms of steady state performance, as evident from Figure 8–9, the GPR is less noisy as compared to NN approach. As observed, the dynamic response of BPNN and GPR is almost similar for chemical mixing tank system. A quantitative analysis of the approaches considered in this work is tabulated in Table 2 for which the results are averaged over 50 simulations. The fault estimation performance quantised in terms of mean square error shows that the MSE value of GPR is less than that of NN. Hence it

can be said that the GPR-based approach offers superior performance as compared to NN-based approach for fault estimation.

Table 2 Case 1: abrupt fault estimation performance analysis

	Mean square error	
Fault	*NN*	*GPR*
Positive fault (+20%)	1.6124	1.4887
Negative fault (–10%)	0.6877	0.5624

4.2 Case study 2

Consider a two phase reactor and condenser system with recycle as shown in Figure 10. In this system, an exothermic reaction occurs between reactant A and reactant B which are fed to the reactor at flow rates F_A and F_B, at temperatures T_A and T_B in vapour and liquid phases, respectively. The rate of diffusion for reactant A in liquid phase is N_{A1} which causes the following exothermic reaction

$$A + B \rightarrow 2C \tag{34}$$

of which reactant B is considered to be non-volatile. Also, the product C of the exothermic reaction diffuses in the vapour phase at rate N_{C1}. With the assumption that the interphase mass-transfer resistance is negligible, the reaction rate in the bulk liquid phase can be expressed as

$$r_A = k_{10} \exp\left(\frac{-E_a}{RT_1}\right) M_1^l \rho x_{A1} x_{B1} \tag{35}$$

where r_a indicates the rate of comsumption of A, k_{10} is pre-exponential factor, E_a is activation energy, T_1 is temperature, ρ is molar density, x_{A1} and x_{B1} indicates mole fractions of reactants A and B respectively. Additionally, the liquid and vapour phases are considered to be ideal mixtures of which the molar density ρ, molar heat capacity c_p and latent heat of vapourisation ΔH^v are constant. From the reactor, the liquid stream is removed from bottom at a constant flow rate F_{1l} while the vapour stream exits from the top at a flow rate F_{1v} and enters the condenser where it is cooled down to temperature T_2. The liquid phase within the condenser is rich with reactant A and thus recycled at a flow rate F_{2l}. The product is in vapour phase and is withdrawn from condenser at flow rate F_{2v} with composition y_{A2}. The DAE model of the system shown in Figure 10 includes differential equations based on mole and overall enthalpy balances while algebraic equations based on interphase mass-transfer rates, ideal gas relations and pressure-drop correlations. The DAE model of two phase reactor and condenser system with recycle is as follows:

$$\dot{M_1^l} = F_B - F_{1l} + F_{2l} + N_{A1} - N_{C1} \tag{36}$$

$$\begin{aligned} \dot{x}_{A1} = \left(\frac{1}{M_1^l}\right) [&-F_B x_{A1} + F_{2l}(x_{A2} - x_{A1}) \\ &+ N_{A1}(1 - x_{A1}) + N_{C1} x_{A1} - r_A] \end{aligned} \tag{37}$$

$$\dot{x}_{B1} = \left(\frac{1}{M_1^l}\right)[F_B(1-x_{B1}) - F_{2l}x_{B1} - N_{A1}x_{B1} + N_{C1}x_{B1} - r_A] \tag{38}$$

$$\dot{M}_1^v = F_A - F_{1v} - N_{A1} + N_{C1} \tag{39}$$

$$\dot{y}_{A1} = \left(\frac{1}{M_1^v}\right)[F_A(1-y_{A1}) - N_{A1}(1-y_{A1}) - N_{C1}y_{A1}] \tag{40}$$

$$\begin{aligned}\dot{T}_1 = \left(\frac{1}{M_1^l + M_1^v}\right)&[F_A(T_A - T_1) + F_B(T_B - T_1) + F_{2l}(T_2 - T_1) \\ &+ \frac{\Delta H^v}{c_p}(N_{A1} - N_{C1}) - \frac{Q_1}{c_p} + r_a\left(\frac{-\Delta H_r}{c_p}\right)\Bigg]\end{aligned} \tag{41}$$

$$\dot{M}_2^l = N_{A2} + N_{C2} - F_{2l} \tag{42}$$

$$\dot{x}_{A2} = \left(\frac{1}{M_2^l}\right)[N_{A2}(1-x_{A2}) - N_{C2}x_{A2}] \tag{43}$$

$$\dot{M}_2^v = F_{1v} - F_{2v} - N_{A2} - N_{C2} \tag{44}$$

$$\dot{y}_{A2} = \left(\frac{1}{M_2^v}\right)[F_{1v}(y_{A1} - y_{A2}) - N_{A2}(1-y_{A2}) + N_{C2}y_{A2}] \tag{45}$$

$$\dot{T}_2 = \left(\frac{1}{M_1^l + M_1^v}\right)\left[F_{1v}(T_1 - T_2) + \frac{\Delta H^v}{c_p}(N_{A2} + N_{C2}) - \frac{Q_2}{c_p}\right] \tag{46}$$

$$0 = N_{A1} - k_A a\left(y_{A1} - \frac{P_{A1}^s x_{A1}}{P_1}\right)\frac{M_1^l}{\rho} \tag{47}$$

$$0 = N_{C1} - k_c a\left(\frac{P_{C1}^s(1 - x_{A1} - x_{B1})}{P_1} - (1 - y_{A1})\right)\frac{M_1^l}{\rho} \tag{48}$$

$$0 = N_{A2} - k_A a\left(y_{A2} - \frac{P_{A2}^s x_{A2}}{P_2}\right)\frac{M_2^l}{\rho} \tag{49}$$

$$0 = N_{C2} - k_c a\left(1 - y_{A2} - \frac{P_{C2}^s(1 - x_{A2})}{P_2}\right)\frac{M_2^l}{\rho} \tag{50}$$

$$0 = P_1\left(V_{1T} - \frac{M_1^l}{\rho}\right) - M_1^v R T_1 \tag{51}$$

$$0 = P_2\left(V_{2T} - \frac{M_2^l}{\rho}\right) - M_2^v R T_2 \tag{52}$$

$$0 = P_1 - P_2 - \frac{1}{0.09}(F_{1v})^{\frac{7}{4}} \tag{53}$$

$$F_{2v} = F_{2v,nom} - K(P_{set} - P_1) \tag{54}$$

Figure 10 Two phase reactor and condenser system with recycle (see online version for colours)

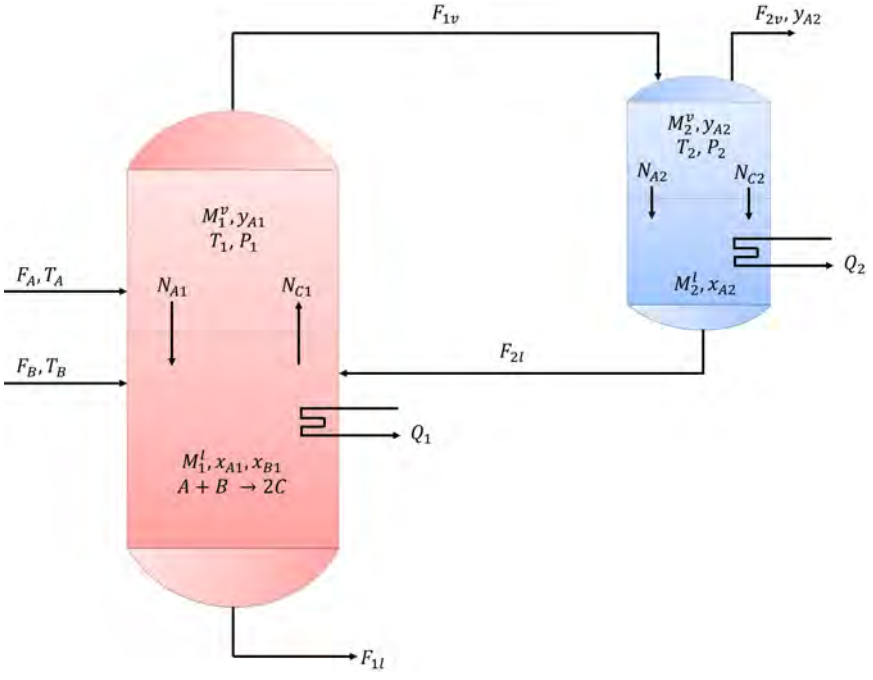

Figure 11 Estimation results (differential states) for two phase reactor and condenser system with recycle (see online version for colours)

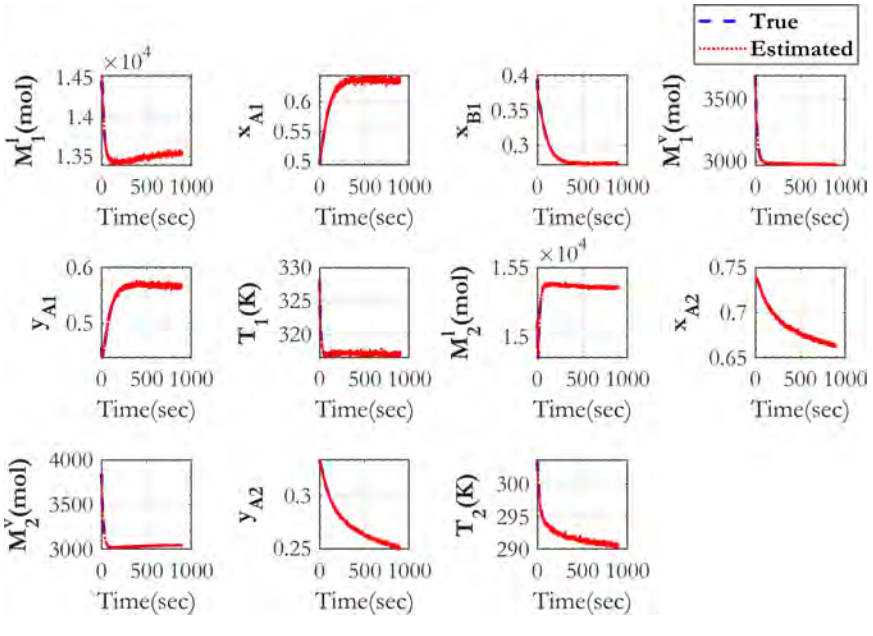

Table 3 Two phase reactor: system parameters and nominal values

Variable	*Description*	*Nominal value*	*Unit*
a	Interfacial mass-transfer area per unit liquid holdup	1,000	m^2/m^3
c_p	Molar heat capacity	80.0	J/molK
E_a	Activation energy	110.0	kJ/mol
F_A	Inlet molar flow rate of reactant A	99.84	mol/s
F_B	Inlet molar flow rate of reactant B	52.0	mol/s
F_{1l}	Molar flow rate of liquid stream from reactor	10.0	mol/s
F_{2l}	Molar flow rate of liquid recycle from condenser to reactor	72.19	mol/s
F_{1v}	Molar flow rate of vapour stream from reactor to condenser	214.03	mol/s
F_{2v}	Molar flow rate of vapour stream from condenser	141.84	mol/s
K	Proportional gain of pressure controller	10.0	mol/s · atm
k_{10}	Pre-exponential factor	2.88e+11	m^3/mol · s
k_A	Overall mass transfer coefficient for A	20	mol/m^2 · s
k_C	Overall mass transfer coefficient for C	30	mol/m^2 · s
M_1^l	Liquid molar hold up in reactor	14.52	kmol
M_2^1	Liquid molar hold up in condenser	15.0	kmol
M_1^v	Vapour molar hold up in reactor	3.75	kmol
M_2^v	Vapour molar hold up in condenser	3.90	kmol
P_1	Pressure in reactor	50.0	atm
P_2	Pressure in condenser	48.69	atm
P_{set}	Setpoint for reactor pressure	50.0	atm
Q_1	Heat output from reactor	863.68	kW
Q_2	Heat output from condenser	1,164.39	kW
T_A	Temperature of feed A	315.0	K
T_B	Temperature of feed B	300.0	K
T_1	Temperature in reactor	330.0	K
T_2	Temperature in condenser	304.16	K
V_{1T}	Volume of reactor	3.0	m^3
V_{2T}	Volume of condenser	3.0	m^3
x_{A1}	Mole fraction of A in liquid phase in reactor	0.49	-
x_{B1}	Mole fraction of B in liquid phase in reactor	0.40	-
x_{A2}	Mole fraction of A in liquid phase in condenser	0.74	-
y_{A1}	Mole fraction of A in vapour phase in reactor	0.47	-
y_{A2}	Mole fraction of A in vapour phase in condenser	0.33	-
ΔH_r	Heat of reaction	–50.0	kJ/mol
ΔH_v	Latent heat of vapourisation	10.0	kJ/mol
ρ	Liquid molar density	15.0	kmol/m^3

In the above equations (47)–(50), P^s_{Ai}, P^s_{Ci} indicates the saturation pressures of A and C in reactor $(i = 1)$ and condenser $(i = 2)$ which can be further expressed as

$$P^s_{Ai} = \exp\left(25.1 - \frac{3{,}400}{T_i + 20}\right) \tag{55}$$

$$P^s_{Ci} = \exp\left(27.3 - \frac{4{,}100}{T_i + 70}\right) \tag{56}$$

Additionally, k_A, k_C denote overall mass transfer coefficients for A and C. The pressure P_1 of the reactor is highly dynamic and can be stabilised by a proportional controller as shown in equation (54) where K is controller gain, P_{set} is desired pressure, F_{2v} is manipulated input and $F_{2v,nom}$ indicates its nominal value. The outputs for the system are $y = \left[T_1\ y_{A2}\ M_2^l\right]^T$ while the inputs are F_A, T_A, F_B, T_B, Q_1, Q_2, F_{2l}.

Figure 12 Estimation results (algebraic states) for two phase reactor and condenser system with recycle (see online version for colours)

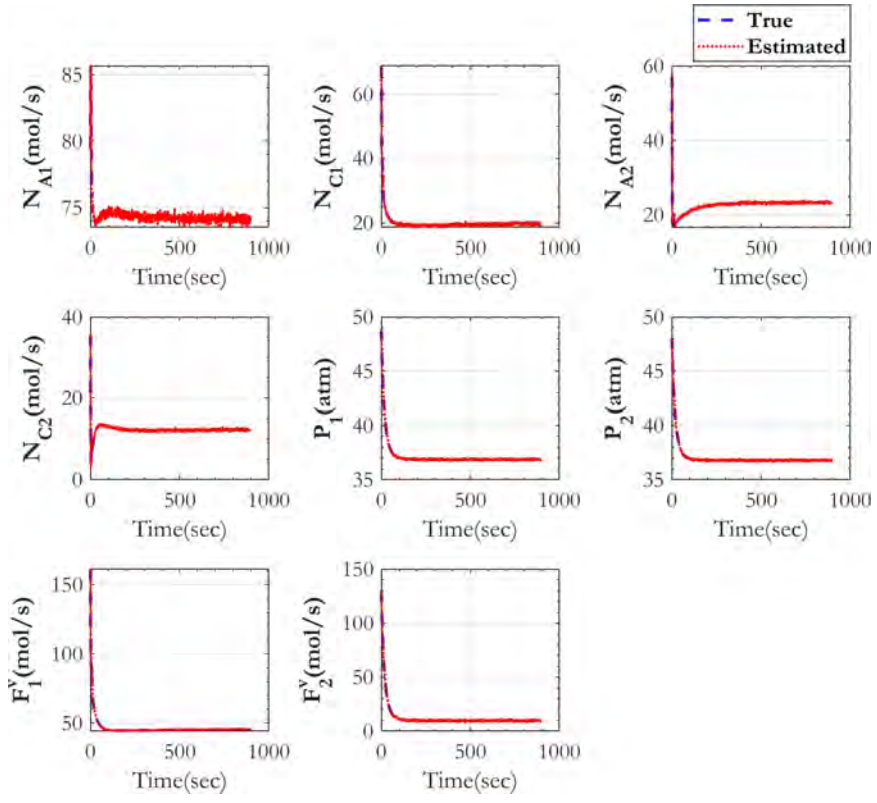

The differential variables for the system are $x_1 = M_1^l$, $x_2 = x_{A1}$, $x_3 = x_{B1}$, $x_4 = M_1^v$, $x_5 = y_{A1}$, $x_6 = T_1$, $x_7 = M_2^l$, $x_8 = x_{A2}$, $x_9 = M_2^v$, $x_{10} = y_{A2}$, $x_{11} = T_2$ while the algebraic variables are considered to be $z_1 = N_{A1}$, $z_2 = N_{C1}$, $z_3 = N_{A2}$, $z_4 = N_{C2}$, $z_5 = P_1$, $z_6 = P_2$, $z_7 = F_{1v}$, $z_8 = F_{2v}$. Firstly, the results of state estimation are put

forth for which the simulation time step $dt = 1s$. The process noise covariance matrix is

$$Q = 10^{(-3)} diag\left(\left[1\,0.1\,0.1\,1\,0.1\,1\,1\,0.1\,1\,0.1\,0.3\right]\right)$$

while the measurement noise covariance matrix is

$$R = 10^{(-3)} diag\left(\left[0.7\,0.1\,0.3\right]\right).$$

Figure 13 Residual evaluation signal vs. threshold: –10% fault in T_B (see online version for colours)

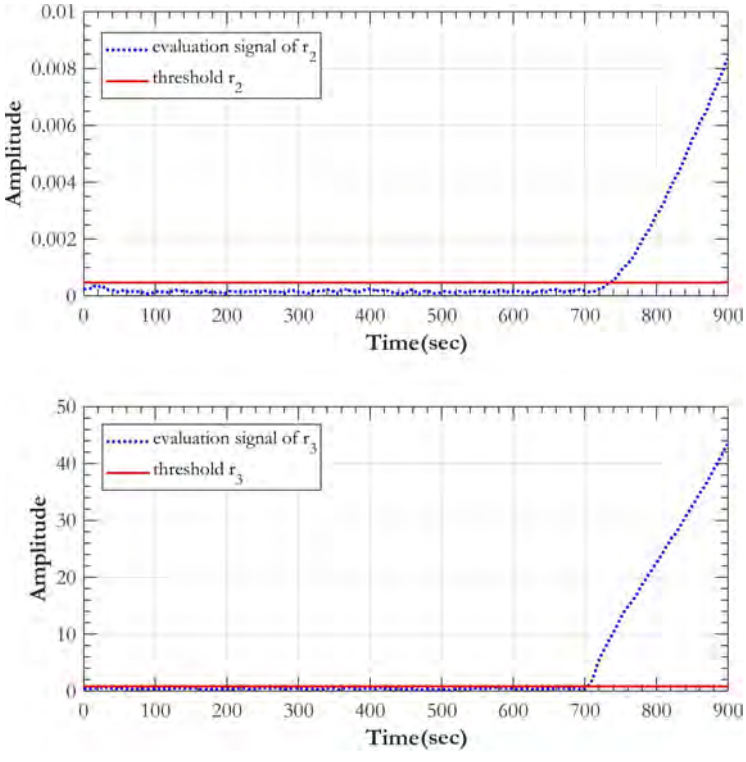

Moreover the initial error covariance matrix is assumed to be $P_0 = I_{19\times19}$. The results of state estimation are presented by Figures 11–12. The differential variables of the state estimation rendered in Figure 11 depict excellent agreement with system states even in dynamic conditions.

As mentioned earlier, the residuals can be generated using system outputs which are obtained with measurement function and state estimates. The residual evaluation function in this case is RMS function and employed in a similar manner as case 1 earlier. In order to analyse the system for fault detection, an input fault in feed temperature of reactant B, i.e., T_B is considered. Upon simulation, it was observed that the fault affected all residuals; however residual r_1 exhibited an inverse response for a brief period ultimately consuming more time to violate its respective threshold level. Since, r_2 and r_3 were also affected by fault, they were considered to determine

fault occurrence. The thresholds were identified from nominal operating conditions to be $[0.00047 \quad 0.8339]^T$. The fault is introduced at time t = 700 s for the simulation results exhibited in Figure 13. The residual evaluation signals are plotted with respective thresholds for the simulation where an input fault of –10% is considered in T_B. As observed, the residual evaluation signals exceeed their respective threshold limits within sometime after the fault is introduced. The residual evaluation signal of r_2 exceeds the threshold at time t = 732 s while of r_3 at time t = 703 s. The fault in T_B can be said to have occurred after the thresholds are violated as shown in Figure 13. Further the fault is confirmed as discussed earlier in case 1 where a window of five time instants is considered. If the fault persists continuously for the considered duration ; the fault is confirmed. For the scenario of Figure 13, the confirmation of fault in T_B is obtained at t = 737 s. Further, the fault estimation approaches are assessed for which the dataset is generated in a manner as described earlier. The dataset contains the information of residuals and fault magnitude (fault in T_B). This dataset so generated is availed by fault estimation approaches under consideration.

Figure 14 Backpropagation neural network structure for fault estimation (for case 2) (see online version for colours)

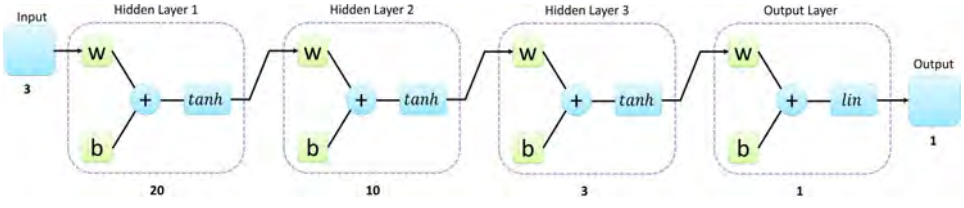

Figure 15 Input (T_B): abrupt fault estimation by NN and GPR approaches (see online version for colours)

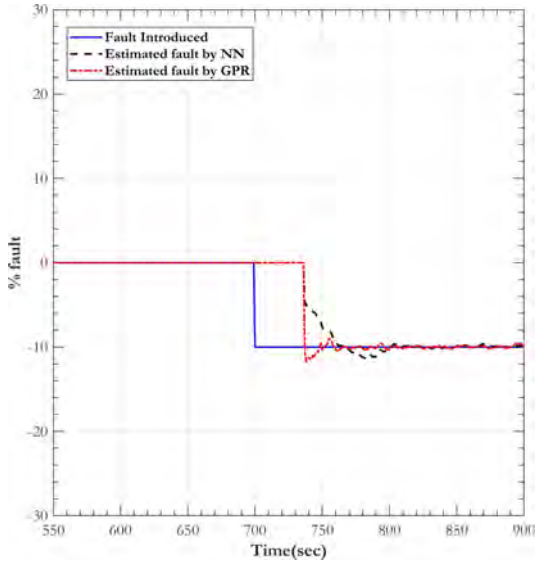

The neural network structure employed for fault estimation is shown in Figure 14. The neural network consists of three hidden layers and one output layer. The first hidden

layer consists of 20 neurons, second hidden layer consists of ten neurons while third hidden layer consists of three neurons with tansigmoidal activation functions. The output layer consists of one neuron which maps to the magnitude of the fault. The dataset generated earlier is provided to this neural network during training. The training of back propagation neural network results in R values of 0.9 which indicates that the network has learned and can predict values close to actual fault magntiudes.

Figure 16 Input (T_B): abrupt fault estimation by NN and GPR approaches (see online version for colours)

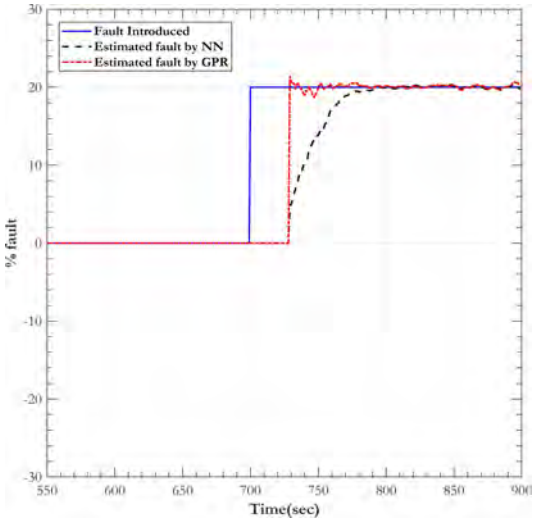

Table 4 Case 2: abrupt fault estimation performance analysis

	Mean square error	
Fault	*NN*	*GPR*
Positive fault (+20%)	15.7468	12.4667
Negative fault (–10%)	4.4249	4.0994

In order to implement the same, this trained neural network is evaluated by applying an abrupt fault in input T_B. Additionally, the GPR model with exponential kernel function is also trained and assessed. The magnitude of the abrupt fault is –10%. The fault is introduced at time t = 700 s while it is detected at time t = 732 s and further, the fault is confirmed at time t = 737 s. The fault is confirmed if the residual evaluation signal exceed their respective thresholds atleast for five consecutive time instants. The fault estimation results for the same are presented in Figure 15 where in the fault introduced is indicated by solid blue line while the estimated faults are indicated by spaced lines. It can be observed that there is some time elapsed before the fault estimation starts. This time difference between the fault introduction and onset of fault estimation includes the time taken for fault detection as well as fault confirmation. Similarly, the fault estimation approaches are analysed for an abrupt fault of 20%. The fault is introduced at time t = 700 s, detected at time t = 724 s and confirmed at time t = 729 s for which the results of

fault estimation are exhibited by Figure 16. On visual inspection, it can be noted that the NN-based approach consumes more time to settle as compared to GPR-based approach. Thus, it is observed that the fault estimation by GPR approach shows better response as compared to NN-based approach. These results corroborate with other observations made earlier.

For the system considered in case 2, a quantitative analysis of fault estimation performance for both approaches is put forth in Table 4. The GPR-based approach shows considerable improvement as compared to NN-based approach of fault estimation. The backpropagation neural network attempts to learn the relation between fault estimates and residuals in a regressive manner and could only moderately generalise as compared to GPR from the dataset offered. However, the GPR model that was trained on the same dataset could establish a relation between fault estimate and noisy residuals because the probabilistic approach allows to consider for variations in the form of distribution. Moreover, in general, the GPR approach learns fewer parameters as compared to neural network. Additonally, GPR approach is a direct approach where new predictions entirely depend upon the training data while NN approach depends on optimisation of parameters from the training data.

5 Conclusions

This study probes various intelligent approaches of fault estimation for NLDSs and demonstrates the same for

1 chemical mixing tank system

2 two phase reactor and condenser system with recycle.

It employs extended Kalman filter for descriptor systems which helps in fault detection while neural network and GPR models are evaluated for fault estimation. The GPR approach presented in this work has hardly been assessed for fault estimation of NLDSs. The approaches considered are demonstrated for abrupt fault estimation and further compared in a quantitative manner so as to evaluate their performance. The results show that RMSE for GPR-based approach improves in the range of 10–20% as compared to NN-based approach for fault estimation. Additionally, in terms of dynamic response, the NN approach shows substandard performance as compared to GPR approach. The GPR approach offers superior performance as compared to NN-based approach inspite of noisy residuals. The fault estimation for GPR model shows excellent performance because of its inherent probabilistic approach.

References

Alkov, I. and Weidemann, D. (2013) 'Fault detection with unscented Kalman filter applied to nonlinear differential-algebraic systems', *2013 18th International Conference on Methods and Models in Automation and Robotics, MMAR 2013*, pp.166–171 [online] http://dx.doi.org/10.1109/mmar.2013.6669900.

Blanke, M., Staroswiecki, M. and Wu, N.E. (2001) 'Concepts and methods in fault-tolerant control', *American Control Conference* [online] http://www.iau.dtu.dk/secretary/pdf/ACCmb30a4.pdf.

Chan, J.C.L., Tan, C.P., Trinh, H. and Kamal, M.A.S. (2019a) 'State and fault estimation for a class of non-infinitely observable descriptor systems using two sliding mode observers in cascade', *Journal of the Franklin Institute*, Vol. 356, No. 5, pp.3010–3029 [online] http://dx.doi.org/10.1016/j.jfranklin.2019.01.044.

Chan, J.C.L., Tan, C.P., Trinh, H., Kamal, M.A.S. and Chiew, Y.S. (2019b) 'Robust fault reconstruction for a class of non-infinitely observable descriptor systems using two sliding mode observers in cascade', *Applied Mathematics and Computation*, Vol. 350, pp.78–92 [online] http://dx.doi.org/10.1016/j.amc.2018.12.071.

Chan, J.C., Tan, C.P., Ooi, J.H. and Trinh, H. (2019c) 'New results in robust fault reconstruction for a class of non-infinitely observable descriptor systems', *Proceedings of the American Control Conference 2019*, July, pp.5058–5064.

Das, M., Sadhu, S. and Ghoshal, T.K. (2014) 'Fault detection and isolation using an adaptive unscented Kalman filter', *IFAC*, Vol. 3 [online] http://dx.doi.org/10.3182/20140313-3-IN-3024.00075.

Fugh, J.N., Marino, M. and Bouklas, N. (2022) 'Local approximate Gaussian process regression for data-driven constitutive models: development and comparison with neural networks', *Computer Methods in Applied Mechanics and Engineering*, Vol. 388, pp.2175–2198.

Hamdi, H., Rodrigues, M., Mechmeche, C., Theilliol, D. and Braiek, N.B. (2012) 'Fault detection and isolation in linear parameter-varying descriptor systems via proportional integral observer', *International Journal of Adaptive Control and Signal Processing*, Vol. 26, No. 3, pp.224–240 [online] http://arxiv.org/abs/LPV_Xiaohang_2015, http://dx.doi.org/10.1002/acs.1260.

Huang, Y., Reklaitis, G.V. and Venkatasubramanian, V. (2003) 'A heuristic extended Kalman filter based estimator for fault identification in a fluid catalytic cracking unit', *Industrial and Engineering Chemistry Research*, Vol. 42, No. 14, pp.3361–3371 [online] http://dx.doi.org/10.1021/ie010659t.

Iqbal, R., Maniak, T., Doctor, F. and Karyotis, C. (2019) 'Fault detection and isolation in industrial processes using deep learning approaches', *IEEE Transactions on Industrial Informatics*, Vol. 15, No. 5, pp.3077–3084 [online] http://dx.doi.org/10.1109/TII.2019.2902274.

Isermann, R. (2005) 'Model-based fault-detection and diagnosis – status and applications', *Annual Reviews in Control*, Vol. 29, No. 1, pp.71–85 [online] http://dx.doi.org/10.1016/j.arcontrol.2004.12.002.

Jia, Q., Chen, W., Zhang, Y. and Li, H. (2015) 'Fault reconstruction and fault-tolerant control via learning observers in Takagi-Sugeno fuzzy descriptor systems with time delays', *IEEE Transactions on Industrial Electronics*, Vol. 62, No. 6, pp.3885–3895 [online] http://dx.doi.org/10.1109/TIE.2015.2404784.

Kamdar, S., Brahmbhatt, H., Patel, T. and Thakker, M. (2015) 'Sensorless speed control of high speed brushed dc motor by model identification and validation', in *2015 5th Nirma University International Conference on Engineering (NUiCONE)*, IEEE, pp.1–6.

Kankar, P.K., Sharma, S.C. and Harsha, S.P. (2011) 'Fault diagnosis of ball bearings using machine learning methods', *Expert Systems with Applications*, Vol. 38, No. 3, pp.1876–1886 [online] http://dx.doi.org/10.1016/j.eswa.2010.07.119.

Kantharia, P., Patel, T. and Thakker, M. (2014) 'Design of sensor fault detection and remote monitoring system for temperature measurement', *International Journal of Current Engineering and Technology*, Vol. 4, No. 2, pp.504–508.

Kumar, A. and Daoutidis, P. (1996) 'Feedback regularization and control of nonlinear differential-Algebraic-equation systems', *AIChE Journal*, Vol. 42, No. 8, pp.2175–2198.

Lee, J., Bahri, Y., Novak, R., Schoenholz, S., Pennington, J. and Sohl-Dickstein, J. (2018) 'Deep neural networks as Gaussian processes', *International Conference on Learning Representations*.

Li, L. (2016) 'Fault detection and fault-tolerant control for nonlinear systems' [online] http://dx.doi.org/10.1007/978-3-658-13020-6.

Mandela, R.K., Rengaswamy, R., Narasimhan, S. and Sridhar, L.N. (2010) 'Recursive state estimation techniques for nonlinear differential algebraic systems', *Chemical Engineering Science*, Vol. 65, No. 16, pp.4548–4556 [online] http://dx.doi.org/10.1016/j.ces.2010.04.020.

Masubuchi, I., Kamitane, Y., Ohara, A. and Suda, N. (1997) 'H infinity control for descriptor systems: a matrix inequalities approach', *Automatica*, Vol. 33, No. 4, pp.669–673 [online] http://dx.doi.org/10.1016/S0005-1098(96)00193-8.

Mohanty, A.R., Pradhan, P.K., Mahalik, N.P. and Dastidar, S.G. (2012) 'Fault detection in a centrifugal pump using vibration and motor current signature analysis', *International Journal of Automation and Control*, Vol. 6, Nos. 3–4, pp.261–276.

Myren, S. and Lawrence, E. (2021) 'A comparison of Gaussian processes and neural networks for computer model emulation and calibration', *Statistical Analysis & Data Mining*, Vol. 14, No. 6, pp.606–623.

Patel, T., Shah, J. and Satria, M. (2013) 'Dynamic modeling, optimal control design and comparison between various control schemes of home refrigerator', *International Journal of Current Engineering and Technology*, pp.2047–2052.

Patel, T., Rao, M., Purohit, J. and Shah, V. (2019) 'Input fault detection using ensemble Kalman filter for nonlinear descriptor systems', *7th Nirma University International Conference on Engineering*.

Patel, T., Rao, M., Purohit, J. and Shah, V. (2020a) 'State estimation of nonlinear descriptor systems using particle swarm optimization based extended Kalman filter', *European Control Conference*.

Patel, T., Rao, M., Purohit, J. and Shah, V. (2020b) 'Kalman filters for descriptor systems applied in domain of fault tolerant control: a review', in Holland, M. (Ed.): *An Introduction to the Extended Kalman Filter*, Chapter 2, Nova Science Publishers, USA.

Purohit, J.L. and Patwardhan, S.C. (2018) 'Development of iterative extended Kalman filter for DAE System', *IFAC-PapersOnLine*, Vol. 51, No. 1, pp.691–696 [online] http://dx.doi.org/10.1016/j.ifacol.2018.05.116.

Qi, G., Zhu, Z., Erqinhu, K., Chen, Y., Chai, Y. and Sun, J. (2018) 'Fault-diagnosis for reciprocating compressors using big data and machine learning', *Simulation Modelling Practice and Theory*, Vol. 80, pp.104–127.

Qiao, L., Zhang, Q. and Zhang, G. (2017) 'Admissibility analysis and control synthesis for T-S fuzzy descriptor systems', *IEEE Transactions on Fuzzy Systems*, Vol. 25, No. 4, pp.729–740 [online] http://dx.doi.org/10.1109/TFUZZ.2016.2574917.

Rao, N.M., Vora, P. and Moudgalya, K.M. (2003) 'PID control of DAE systems', *Industrial and Engineering Chemistry Research*, Vol. 42, No. 20, pp.4599–4610 [online] http://dx.doi.org/10.1021/ie0208671.

Schulz, E., Speekenbrink, M. and Krause, A. (2018) 'A tutorial on Gaussian process regression: modelling, exploring, and exploiting functions', *Journal of Mathematical Psychology*, Vol. 85, pp.1–16 [online] http://dx.doi.org/10.1016/j.jmp.2018.03.001.

Shi, F. and Patton, R.J. (2014) 'Simultaneous state and fault estimation for descriptor systems using an augmented PD observer', in *IFAC Proceedings Volumes (IFAC-PapersOnline)*, IFAC, Vol. 19, pp.8006–8011 [online] http://dx.doi.org/10.3182/20140824-6-ZA-1003.01383.

Singhal, R., Kumar, R. and Neeli, S. (2022) 'Residual-based fault detection isolation and recovery of a greenhouse', *International Journal of Automation and Control*, Vol. 16, Nos. 3–4, pp.410–432.

Sjöberg, J. (2006) *Some Results on Optimal Control for Nonlinear Descriptor Systems*, Doctoral dissertation, Institutionen för systemteknik.

Sun, T., Yu, G., Gao, M., Zhao, L., Bai, C. and Yang, W. (2021) 'Fault diagnosis methods based on machine learning and its applications for wind turbines: a review', *IEEE Access*, Vol. 9, pp.147481–147511.

Taqvi, S.A., Tufa, L.D., Zabiri, H., Maulud, A.S. and Uddin, F. (2018) 'Fault detection in distillation column using NARX neural network', *Neural Computing and Applications*, Vol. 32, No. 8, pp.3503–3519 [online] http://dx.doi.org/10.1007/s00521-018-3658-z.

Vemuri, A.T., Polycarpou, M.M. and Ciric, A.R. (2001) 'Fault diagnosis of differential-algebraic systems', *IEEE Transactions on Systems, Man, and Cybernetics Part A: Systems and Humans*, Vol. 31, No. 2, pp.143–152 [online] http://dx.doi.org/10.1109/3468.911372.

Wang, Z., Rodrigues, M., Theilliol, D. and Shen, Y. (2013) 'Actuator fault estimation observer design for discrete-time linear parameter-varying descriptor systems', *International Journal of Adaptive Control and Signal Processing*, Vol. 22, No. 4, pp.325–343 [online] http://arxiv.org/abs/LPV_Xiaohang_2015, http://dx.doi.org/10.1002/acs.

Wang, Z., Shen, Y. and Zhang, X. (2014) 'Actuator fault estimation for a class of nonlinear descriptor systems', *International Journal of Systems Science*, Vol. 45, No. 3, pp.487–496 [online] http://dx.doi.org/10.1080/00207721.2012.724100.

Wang, Z., Liu, X., Zhang, W., Zhi, Y. and Cheng, S. (2022) 'The statistical analysis in the era of big data', *International Journal of Modelling, Identification and Control*, Vol. 40, No. 2, pp.151–157.

Witczak, M., Buciakowski, M., Puig, V., Rotondo, D. and Nejjari, F. (2016) 'An LMI approach to robust fault estimation for a class of nonlinear systems', *International Journal of Robust and Nonlinear Control*, Vol. 26, No. 7, pp.1530–1548 [online] http://arxiv.org/abs/arXiv:1505.02595v1, http://dx.doi.org/10.1002/rnc.3365.

Wu, J., Huang, Z., Guan, Y., Cai, C., Wang, Q., Xiao, Z., Zheng, Z., Zhang, H. and Zhang, X. (2011) 'An intelligent environmental monitoring system based on autonomous mobile robot', *2011 IEEE International Conference on Robotics and Biomimetics, ROBIO 2011*, Vol. 26, No. 3, pp.138–143 [online] http://dx.doi.org/10.1109/ROBIO.2011.6181275.

Yeu, T-K., Kim, H-S. and Kawaji, S. (2008) 'Fault detection, isolation and reconstruction for descriptor systems', *Asian Journal of Control*, Vol. 7, No. 4, pp.356–367 [online] http://dx.doi.org/10.1111/j.1934-6093.2005.tb00398.x.

Zhang, Y. and Jiang, J. (2003) 'Bibliographical review on reconfigurable fault-tolerant control systems', *IFAC Proceedings Volumes (IFAC-PapersOnline)*, Vol. 36, No. 5, pp.257–268 [online] http://dx.doi.org/10.1016/S1474-6670(17)36503-5.

Zhang, X., Polycarpou, M.M. and Parisini, T. (2002) 'A robust detection and isolation scheme for abrupt and incipient faults in nonlinear systems', *IEEE Transactions on Automatic Control*, Vol. 47, No. 4, pp.576–593 [online] http://dx.doi.org/10.1109/9.995036.

Zhang, K., Jiang, B. and Cocquempot, V. (2008) 'Adaptive observer-based fast fault estimation', *International Journal of Control, Automation and Systems*, Vol. 6, No. 3, pp.320–326.